Chemical Engineering Science 65 (2010) 3088–3099

Contents lists available at ScienceDirect

Chemical Engineering Science

journal homepage: www.elsevier.com/locate/ces

Thermodynamic modeling of confined fluids using an extension of the generalized van der Waals theory ☆

Leonardo Travalloni [a], Marcelo Castier [a,b,*], Frederico W. Tavares [a], Stanley I. Sandler [c]

[a] Escola de Química, Universidade Federal do Rio de Janeiro, C.P. 68542, CEP 21949-900, Rio de Janeiro, RJ, Brazil
[b] Department of Chemical and Petroleum Engineering, United Arab Emirates University, P.O. Box 17555, Al Ain, United Arab Emirates
[c] Department of Chemical Engineering, University of Delaware, 19716-3110, Newark, DE, USA

ARTICLE INFO

Article history:
Received 11 August 2009
Received in revised form
12 January 2010
Accepted 28 January 2010
Available online 4 February 2010

Keywords:
Adsorption
Porous media
Mathematical modeling
Statistical thermodynamics
State equation

ABSTRACT

Based on the generalized van der Waals theory, a cubic equation of state (the van der Waals equation) was extended to describe the behavior of pure fluids and mixtures confined in porous solids. Each pore was assumed to be a cylinder with a continuous and homogeneous surface. Fluid molecules were assumed spherical, interacting with each other and with the wall of the pore through square-well potentials. Pairwise additivity was assumed for the attractive parts of all interaction potentials. The repulsive part of the equation of state for confined fluids was modeled based on literature data for the packing of hard spheres in cylinders. The effect of pore size on fluid properties was explicitly represented in the model, allowing its application to both confined and bulk fluids thus providing a consistent description of adsorption systems for all pore sizes. The resulting equation of state has two fitting parameters for each component of the fluid, which are related to the interaction between the fluid molecules and the pore walls. Calculations of pure fluid adsorption were carried out in order to analyze the sensitivity of the model to its fitting parameters and to pore size. It was found that the model is able to describe different types of adsorption isotherms. The model correlated experimental data of pure fluid adsorption quite well and was then used to predict the adsorption of several binary mixtures and one ternary mixture with no additional fitting, with good results. The methodological framework presented here can be extended to other widely used equations of state for modeling confined fluids.

1. Introduction

The properties of a fluid confined in microscopic spaces, as in the cavities of a porous solid, may differ significantly from those of the bulk fluid due to the interaction between the molecules of the fluid and the solid surface. The effect of confinement on fluid properties becomes more pronounced as the dimensions of the confining space decrease. The ability to correlate and predict this effect is important in applications such as the modeling of oil reservoirs, in which the fluid is confined in porous rocks, and more generally other adsorption phenomena, including separation processes that may be strongly influenced by the heterogeneity of most adsorbents. However, common adsorption models do not explicitly include the effect of adsorbent pore size and shape, and represent only the chemical heterogeneity of the solid surface, limiting the understanding of adsorption on solids with large pore size distributions.

Among the several approaches to model fluids confined in idealized pores, the most complete can describe the local properties of the confined fluid in detail. These include molecular simulations (Coasne et al., 2009; Demontis et al., 2003; Dukovski et al., 2000; Giovambattista et al., 2009; Jiang and Sandler, 2006; Nicholson and Parsonage, 1982; Severson and Snurr, 2007) and density functional theory (Kotdawala et al., 2005; Wu, 2006). However, these approaches demand great computational effort, hindering their application to more complex problems, such as the distribution of a fluid mixture in a heterogeneous porous matrix. It is therefore of use to develop simpler models that can describe confined fluid behavior in less detail, but with sufficient accuracy for predictive calculations. Nevertheless, for a better representation of the microscopic and macroscopic behavior of confined fluids, more sophisticated techniques such as molecular simulations are necessary.

When knowledge of the global properties of a confined fluid is sufficient, an analytical equation of state is among the easiest ways to calculate these properties. Such an equation of state must represent the main effects of confinement explicitly, i.e., the effect of pore size and of the interaction between the fluid molecules and the pore wall (molecule–wall interaction). In this way, the same equation of state can describe the fluid behavior from the

☆ Funded by BZG.
* Corresponding author at: Department of Chemical and Petroleum Engineering, United Arab Emirates University, P.O. Box 17555, Al Ain, United Arab Emirates. Tel.: +971 3 7133634; fax: +971 3 7624262.
E-mail addresses: castier@eq.ufrj.br, mcastier@uaeu.ac.ae (M. Castier).

0009-2509/$ - see front matter © 2010 Elsevier Ltd. All rights reserved.
doi:10.1016/j.ces.2010.01.032

bulk state to extreme confinement. This is the approach adopted in this work.

Previous work on this approach includes that of Zhu et al. (1999), who developed an equation of state for fluids confined in cylindrical mesopores based on the thermodynamic interface theory. That model described the adsorption of nitrogen on MCM-41 samples with different pore sizes.

Schoen and Diestler (1998) extended the van der Waals equation of state to fluids confined in slit pores based on the perturbation theory. A hard sphere fluid of uniform density was taken as reference and a correction related to attractive interactions was added using the mean field approximation. The model could predict some qualitative effects of confinement in mesopores, such as capillary condensation and the reduction in the critical temperature of the fluid. However, the performance of the model near the critical point of the bulk fluid was unsatisfactory, probably due to the assumption of a uniform reference fluid. To improve the model performance, the authors suggested that one should consider the separate contributions of distinct pore regions, taken as a function of the distance from the wall, as indicated by molecular simulation results. Giaya and Thompson (2002) extended the methodology of Schoen and Diestler (1998) to cylindrical pores, obtaining good predictive results for water adsorption on two different mesoporous solids.

Zarragoicoechea and Kuz (2002, 2004) extended the van der Waals equation of state to fluids confined in pores with square cross section, based on a classical thermodynamics formulation and on the assumption that the confined fluid pressure has a tensorial character. The attractive molecule–wall interaction was neglected. The model predicted capillary condensation conditions that were consistent with numerical simulation results. Moreover, calculations of critical temperatures for several fluids confined in MCM-41 samples with different pore sizes were in good agreement with experimental data with no fitting of model parameters.

Derouane (2007) proposed a simple modification of the attractive part of the van der Waals equation of state to extend this model to fluids confined in microporous solids far from pore saturation. A term dependent on pore size was added to the original model to represent the increase in the fluid pressure due to the molecule–wall interaction. The short-range repulsive effect of confinement was neglected. The model described qualitatively the reduction of both the critical temperature and the critical volume of the fluid with pore size reduction, in agreement with experimental findings (Schoen and Diestler, 1998).

In this work, we extend the van der Waals equation of state to the modeling of pure fluids and mixtures confined in porous solids. The van der Waals model was chosen because it is simple and capable of describing the qualitative behavior of most pure fluids and mixtures. As such, it is a suitable starting point to evaluate the new approach we propose to extend widely used equations of state to the modeling of confined fluids. The model development is guided by the generalized van der Waals theory (Lee et al., 1985; Sandler, 1985). The goal is to derive an equation of state suitable to both confined and bulk fluids, thus providing a consistent description of adsorption systems. Further, though the van der Waals equation is used here, the proposed methodology is easily extended to more complicated equations of state.

2. Model

The properties of a fluid mixture can be obtained from the following form of the canonical partition function (Hill, 1960):

$$Q(T,V,N_1,N_2,\ldots,N_{NC}) = \prod_{i=1}^{NC}\left(\frac{q_{int,i}^{N_i}}{\lambda_i^{3N_i}N_i!}\right)V_f^N \exp\left(\int_\infty^T \frac{E_{conf}}{kT^2}\,dT\right) \quad (1)$$

where T is the absolute temperature, V is the total volume of the system, NC is the number of components of the mixture, N_i is the number of molecules of component i, $q_{int,i}$ is the internal partition function of one molecule of component i, λ_i is the de Broglie wavelength of component i, V_f is the free volume, E_{conf} is the configurational energy, k is the Boltzmann constant, and N is the total number of molecules of the mixture:

$$N = \sum_{i=1}^{NC} N_i \quad (2)$$

The basis of several cubic equations of state is to develop expressions for V_f and E_{conf} assuming the fluid molecules are spheres that interact with each other through the square-well potential:

$$u_{ij}(r_{ij}) = \begin{cases} +\infty, & r_{ij} < \sigma_{ij} \\ -\varepsilon_{ij}, & \sigma_{ij} \le r_{ij} \le (\sigma_{ij}+\delta_{ij}) \\ 0, & r_{ij} > (\sigma_{ij}+\delta_{ij}) \end{cases} \quad (3)$$

where r_{ij} is the distance between the mass centers of one molecule of component i and one molecule of component j, ε_{ij} is the energy parameter of the interaction between these molecules, δ_{ij} is the square-well width of this interaction, and σ_{ij} is the average molecular diameter for the interacting components i and j.

2.1. Free volume: pure fluids

Several cubic equations of state are based on the following simple expression for the free volume:

$$V_f = V - N\beta = V - \frac{N}{\rho_{max}} \quad (4)$$

where β is the excluded volume per fluid molecule and ρ_{max} is the molecular density of the close-packed fluid, and both are constants for each bulk fluid. For a confined fluid, however, ρ_{max} is a function of the confinement dimensions, due to the formation of a structured layer of fluid molecules near each solid wall. In the case of adsorption, ρ_{max} is a function of the pore size of the adsorbent. Assuming the adsorbent pores are cylinders of radius r_p and the fluid molecules are spheres of diameter σ, ρ_{max} is a function of the r_p/σ ratio. From the analytical and experimental data of mean porosity (ξ) of loosely packed beds of hard spheres in cylinders for different r_p/σ ratios, compiled by Mueller (2005), we obtained a good fit (Fig. 1) of this functional dependence using the expression:

$$\xi = c_1 + c_2\exp\left(c_3\left(0.5-\frac{r_p}{\sigma}\right)\right) - c_4\exp\left(c_5\left(0.5-\frac{r_p}{\sigma}\right)\right) \quad (5)$$

where c_1=0.393684, c_2=0.250942, c_3=0.620861, c_4=0.311601, and c_5=4.01377. The expression for ρ_{max} then is

$$\rho_{max}\sigma^3 = \frac{6}{\pi}(1-\xi) = \frac{6}{\pi}\left(1-c_1-c_2\exp\left(c_3\left(0.5-\frac{r_p}{\sigma}\right)\right) + c_4\exp\left(c_5\left(0.5-\frac{r_p}{\sigma}\right)\right)\right) \quad (6)$$

In Eq. (6), when $r_p/\sigma \to \infty$ (bulk fluid), $\rho_{max}\sigma^3 \to 1.15798$. For consistency between Eq. (6) and the van der Waals equation of state model, this limit must be taken into account in the calculation of the fluid molecule effective diameter:

$$\sigma = \sqrt[3]{1.15798\beta} = \sqrt[3]{1.15798\frac{b}{N_{av}}} \quad (7)$$

where b is the volume parameter of the van der Waals equation of state and N_{av} is the Avogadro number. Eq. (7) predicts σ values similar to those obtained from viscosity data (Poling et al., 2000)

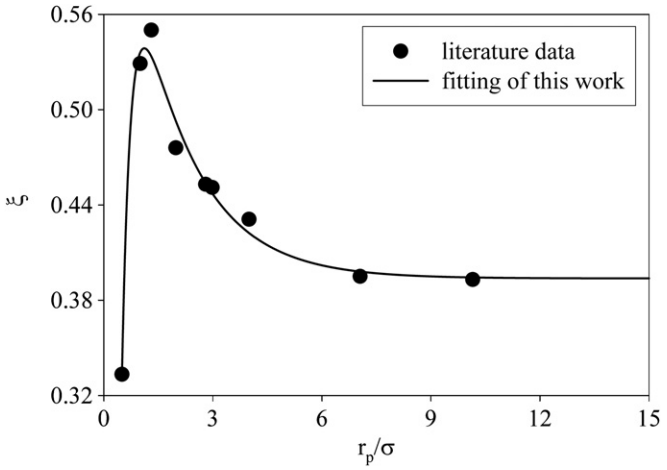

Fig. 1. Fitting of literature mean porosity data using Eq. (5).

for some compounds modeled by the Lennard-Jones potential, such as *n*-alkanes with one to six carbon atoms, benzene, and the inorganic gases N_2, O_2, and CO_2 (with deviations of up to 6%, except for *n*-butane, which has a deviation of 17%). However, the predictions of Eq. (7) are in lesser agreement with the σ values obtained from second-virial coefficient data (Prausnitz et al., 1999), with deviations of up to 35%.

2.2. Free volume: mixtures

Assuming additivity for the hardcore contributions of all components and following the analysis above, the free volume of the fluid mixture is modeled by the following expression:

$$V_f = V - \sum_{i=1}^{NC} \left(\frac{N_i}{\rho_{max,i}} \right) \tag{8}$$

where $\rho_{max,i}$ is the molecular density of pure component i in a packed structure, calculated from Eq. (6).

2.3. Configurational energy: pure fluids

The configurational energy of a bulk fluid is related to the molecule–molecule interactions that occur throughout the system volume. For a confined fluid, however, a model for E_{conf} must also take into account the interactions between the fluid molecules and the wall of the pore that confines the fluid (molecule–wall interactions). Assuming that these interactions also occur through a square-well potential, there are three regions inside each pore, as shown in Fig. 2, where δ_p is the square-well width of the molecule–wall interaction potential. These regions were considered only for the computation of the attractive contributions to the model, since we are interested in describing the confined fluid as a global phase.

Region I is beyond the reach of the attractive field of the pore wall; therefore, only molecule–molecule interactions need to be considered in this region. In region II (the square-well region of the pore), fluid molecules are subjected to the field of the wall, so both molecule–molecule and molecule–wall interactions need to be computed. Region III is inaccessible to the mass centers of the fluid molecules due to the hardcore repulsion imposed by the wall.

The van der Waals configurational energy of bulk fluids is based on the hypothesis of pairwise additivity for the attractive part of the molecule–molecule interaction potential. Extending this hypothesis to the attractive part of the molecule–wall interaction potential, the configurational energy of a confined pure fluid is

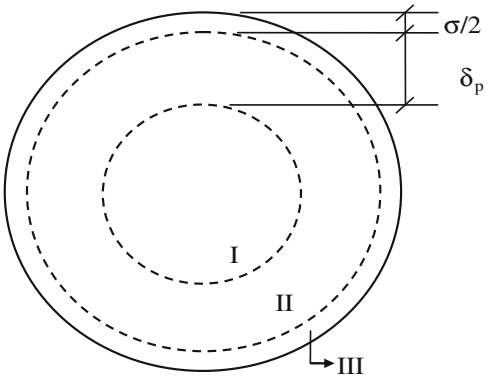

Fig. 2. Regions inside a cylindrical pore, defined by the molecule–wall interaction potential as a function of the distance from the wall.

$$E_{conf} = -\frac{N}{2} N_c \varepsilon - N F_p \varepsilon_p \tag{9}$$

where N_c is the molecule–molecule coordination number, ε is the energy parameter of the molecule–molecule interaction, ε_p is the energy parameter of the molecule–wall interaction, and F_p is the fraction of the confined fluid molecules that occupy the square-well region of the pores (i.e. the fraction of the confined molecules that interact with the solid walls). In Eq. (9), the first term is the van der Waals configurational energy, which results from molecule–molecule interactions taking place in regions I and II of Fig. 2, and the second term results from molecule–wall interactions taking place in region II. Also, it is assumed that each fluid molecule in the square-well region of a pore interacts globally with the wall of that pore, which is taken as a continuous and homogeneous surface. The edge effect of the pore on the molecule–wall interaction potential was neglected.

In the derivation of the van der Waals equation of state, N_c is assumed to be a linear function of fluid density. For a confined fluid, however, N_c also depends on the r_p/σ ratio, since the fluid structure becomes one-dimensional when the confinement degree reaches its maximum (i.e., the upper limit of N_c is only 2 when $r_p/\sigma \to 0.5$). In order to satisfy this limit, a geometric factor was introduced in the expression of the van der Waals molecule–molecule coordination number:

$$N_c = c\rho \left(1 - \frac{2}{5} \frac{\sigma}{r_p} \right) \tag{10}$$

where c is a constant and ρ is the average molecular density of the confined fluid. The geometric factor in parentheses in Eq. (10) was formulated assuming 10 as the maximum N_c of bulk fluids (Prausnitz et al., 1999). When $r_p/\sigma \to \infty$ (bulk fluid), Eq. (10) reduces to the van der Waals linear function ($N_c = c\rho$). When $r_p/\sigma \to 0.5$ (maximum confinement), the geometric factor results in a reduction of the van der Waals coordination number by a factor of 5, leading to a maximum value of about 2 for N_c in the one-dimensional fluid.

In Eq. (9), F_p represents a simplified way to account for the local distribution of the fluid molecules inside each pore. This distribution is a complex function of temperature, fluid density, confinement degree, and the interaction potentials assumed for the molecule–molecule and molecule–wall interactions. To avoid the demanding theoretical problem of finding the confined fluid local distribution, the following empirical expression was used to

model F_p:

$$F_p = F_{pr} + (1-F_{pr})\left(1-\exp\left(-\frac{\varepsilon_p}{kT}\right)\right)\left(1-\frac{\rho}{\rho_{max}}\right)^{\theta} \tag{11}$$

where F_{pr} is the fraction of the confined molecules in the square-well region of the pores for random distribution of the fluid. This fraction is the ratio between the volume of region II in Fig. 2 and the pore volume accessible to the mass centers of the fluid molecules (i.e., the sum of the volumes of regions I and II):

$$F_{pr} = \frac{(r_p-\sigma/2)^2-(r_p-\sigma/2-\delta_p)^2}{(r_p-\sigma/2)^2} \tag{12}$$

Eq. (11) satisfies different physical limits of the confined fluid: when $\rho\to\rho_{max}$ or $T\to\infty$, the fluid is randomly distributed inside the pores (F_p=F_{pr}); when $\rho\to 0$ and $T\to 0$, all the confined molecules occupy the square-well region of the pores (F_p=1). In this way, the model represents the higher probability of finding fluid molecules close to the pore wall due to its attractive field.

In Eq. (11), θ is a geometric term that modulates the effect of ρ on F_p according to the confinement degree. Comparing two pores with the same values of ρ and length, but different values of r_p, there will be more molecules confined in the larger pore than in the smaller one, though the square-well regions of both have the same width. Therefore, as ρ increases, the square-well region reaches saturation at a lower value of ρ in the larger pore. As a consequence, the fluid is randomly distributed at lower densities in larger pores. In order to represent that behavior, the following expression was chosen for θ:

$$\theta = \frac{r_p}{\delta_p+\sigma/2} \tag{13}$$

Fig. 3 shows the effect of density on fluid distribution inside a pore for different values of θ (the effect of temperature was omitted, for simplicity). As θ increases, the confined fluid distribution becomes less sensitive to the variation of ρ near ρ_{max}. Consequently the random distribution is favored as r_p increases, which is expected due to the smaller effect of the molecule–wall interactions.

2.4. Configurational energy: mixtures

Assuming the hypothesis of pairwise additivity for the attractive parts of all molecule–molecule and molecule–wall interaction potentials, the extension of Eq. (9) to mixtures is as follows:

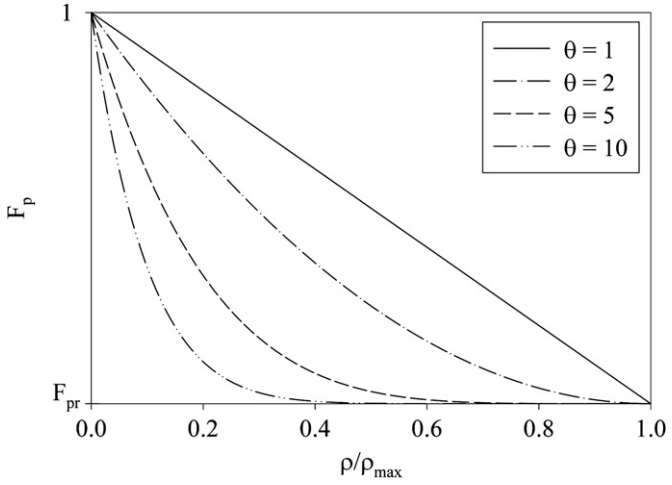

Fig. 3. Effect of density on fluid distribution inside a pore (for $T\to 0$ or $\varepsilon_p\to\infty$).

$$E_{conf} = -\sum_{i=1}^{NC}\sum_{j=1}^{NC}\left(\frac{N_j}{2}N_{c,ij}\varepsilon_{ij}\right)-\sum_{i=1}^{NC}(N_iF_{p,i}\varepsilon_{p,i}) \tag{14}$$

where $N_{c,ij}$ is the number of molecules of component i around a central molecule of component j, $F_{p,i}$ is the fraction of the confined molecules of component i that interact with the solid walls, $\varepsilon_{p,i}$ is the energy parameter of the molecule–wall interaction for component i, and ε_{ij} is given by the combining rule:

$$\varepsilon_{ij} = \sqrt{\varepsilon_{ii}\varepsilon_{jj}} \tag{15}$$

where ε_{ii} is the energy parameter of the interaction between two molecules of component i. In analogy with Eq. (10), the molecule–molecule coordination number of the confined mixture is

$$N_{c,ij} = cx_i\rho\left(1-\frac{2}{5}\frac{\sigma_{ij}}{r_p}\right) \tag{16}$$

where x_i is the mole fraction of component i and σ_{ij} is given by the combining rule:

$$\sigma_{ij} = \frac{\sigma_i+\sigma_j}{2} \tag{17}$$

where σ_i is the molecular diameter of component i, calculated with Eq. (7) from the van der Waals volume parameter of that component (b_i). The distribution of the molecules of each component i inside the pores was modeled by an expression analogous to that proposed for pure fluids:

$$F_{p,i} = F_{pr,i} + (1-F_{pr,i})\left(1-\exp\left(-\frac{\varepsilon_{p,i}}{kT}\right)\right)\left(1-\frac{x_i\rho}{\rho_{max,i}}\right)^{\theta_i} \tag{18}$$

with

$$F_{pr,i} = \frac{(r_p-\sigma_i/2)^2-(r_p-\sigma_i/2-\delta_{p,i})^2}{(r_p-\sigma_i/2)^2} \tag{19}$$

and

$$\theta_i = \frac{r_p}{\delta_{p,i}+\sigma_i/2} \tag{20}$$

where $\delta_{p,i}$ is the square-well width of the molecule–wall interaction potential for component i. Eq. (18) has the assumption that the distribution of each component inside the pores is not affected by the presence of the other components, which is a limitation when modeling asymmetric mixtures.

2.5. Equation of state

The equation of state of the confined fluid mixture and the chemical potential of each component i are analytically obtained from the expression we have derived for the canonical partition function using the thermodynamic relations (Hill, 1960):

$$P = kT\left(\frac{\partial(\ln Q)}{\partial V}\right)_{T,N_1,N_2,\ldots,N_{NC}} \tag{21}$$

$$\mu_i = -kT\left(\frac{\partial(\ln Q)}{\partial N_i}\right)_{T,V,N_{j\neq i}} \tag{22}$$

Using the van der Waals expression for the energy parameter of each interaction between identical molecules:

$$\varepsilon_{ii} = \frac{2a_i}{cN_{av}^2} \tag{23}$$

and changing the molecular variables to a molar basis, the final expressions of the equation of state of the confined mixture and

the chemical potential of component i are

$$P=\frac{RT}{v-b_p}-\frac{a_p}{v^2}-\sum_{i=1}^{NC}\left(x_i\theta_i\frac{x_ib_{p,i}}{v^2}\left(1-\frac{x_ib_{p,i}}{v}\right)^{\theta_i-1}(1-F_{pr,i})\times\left(RT\left(1-\exp\left(-\frac{N_{av}\varepsilon_{p,i}}{RT}\right)\right)-N_{av}\varepsilon_{p,i}\right)\right) \tag{24}$$

$$\mu_i=\mu_{0,i}+RT\left(\ln\left(\frac{N_{av}x_i\lambda_i^3}{v-b_p}\right)+\left(\frac{b_{p,i}}{v-b_p}\right)\right)-\frac{2}{v}\sum_{j=1}^{NC}\left(x_j\sqrt{a_ia_j}\left(1-\frac{2}{5}\frac{\sigma_{ij}}{r_p}\right)\right)-F_{pr,i}N_{av}\varepsilon_{p,i}+\left(1-(\theta_i+1)\frac{x_ib_{p,i}}{v}\right)\left(1-\frac{x_ib_{p,i}}{v}\right)^{\theta_i-1}(1-F_{pr,i})\times\left(RT\left(1-\exp\left(-\frac{N_{av}\varepsilon_{p,i}}{RT}\right)\right)-N_{av}\varepsilon_{p,i}\right) \tag{25}$$

where R is the gas constant, v is the average molar volume of the confined mixture, $\mu_{0,i}$ is the reference chemical potential of component i (related to the intramolecular contribution to the partition function), $F_{pr,i}$ and θ_i are computed in Eqs. (19) and (20), respectively, a_p and b_p are the modified van der Waals parameters for the mixture, which depend on the confinement degree through the expressions:

$$a_p=\sum_{i=1}^{NC}\sum_{j=1}^{NC}\left(x_ix_j\sqrt{a_ia_j}\left(1-\frac{2}{5}\frac{\sigma_{ij}}{r_p}\right)\right) \tag{26}$$

$$b_p=\sum_{i=1}^{NC}x_ib_{p,i} \tag{27}$$

and $b_{p,i}$ is the van der Waals volume parameter of component i modified by confinement, given by

$$b_{p,i}=\frac{N_{av}}{\rho_{max,i}} \tag{28}$$

where $\rho_{max,i}$ is computed from Eq. (6). The model presented above has, for each component of the confined fluid, two parameters that characterize the molecule–wall interactions ($\varepsilon_{p,i}$ and $\delta_{p,i}$), in addition to the known parameters of the original van der Waals equation of state model (a_i and b_i) that characterize each fluid component. The molecule–wall interaction parameters depend only on the chemical nature of the solid and of each fluid component, and can be fitted from experimental data of pure fluid adsorption. With estimated values for the molecule–wall interaction parameters of all fluid components, the model can be used in predictive calculations of mixture adsorption. Furthermore, once the molecule–wall interaction parameters had been estimated for a given temperature, the adsorption behavior of the fluid in other temperatures could be calculated without any additional effort. This is an advantage of the proposed model compared to common adsorption models, which need to be readjusted to a different experimental data set to represent each particular condition. The pure fluid versions of Eqs. (24) and (25) are obtained by setting $NC=1$:

$$P=\frac{RT}{v-b_p}-\frac{a_p}{v^2}-\theta\frac{b_p}{v^2}\left(1-\frac{b_p}{v}\right)^{\theta-1}(1-F_{pr})\left(RT\left(1-\exp\left(-\frac{N_{av}\varepsilon_p}{RT}\right)\right)-N_{av}\varepsilon_p\right) \tag{29}$$

$$\mu=\mu_0+RT\left(\ln\left(\frac{N_{av}\lambda^3}{v-b_p}\right)+\left(\frac{b_p}{v-b_p}\right)\right)-\frac{2a_p}{v}-F_{pr}N_{av}\varepsilon_p+\left(1-(\theta+1)\frac{b_p}{v}\right)\left(1-\frac{b_p}{v}\right)^{\theta-1}(1-F_{pr})\left(RT\left(1-\exp\left(-\frac{N_{av}\varepsilon_p}{RT}\right)\right)-N_{av}\varepsilon_p\right) \tag{30}$$

When $r_p\to\infty$ (bulk fluid), Eq. (24) reduces to the van der Waals equation of state with classical mixing and combining rules for parameters a_i and b_i. Therefore, the model of this work can describe the average behavior of a fluid mixture from the bulk state to extreme confinement using a single set of parameters for each combination of fluid compounds and a single adsorbent solid. Also, considering a fluid confined in multiple pores, as those of an adsorbent solid, the large number of fluid molecules present in these pores does satisfy the thermodynamic limit, allowing the use of our model together with the classical thermodynamics formulation.

3. Calculations of pure fluid adsorption using the model

The condition for the adsorption equilibrium of a pure fluid is

$$\mu_b(T,P_b;a,b)=\mu_a(T,\rho_a,r_p;a,b,\varepsilon_p,\delta_p) \tag{31}$$

where μ_b and P_b are the bulk phase chemical potential and pressure, respectively, and μ_a and ρ_a are the adsorbed phase chemical potential and density, respectively. In each adsorption calculation, the temperature of the system, the bulk phase pressure, the pore radius of the adsorbent (and its total pore volume), parameters a, b, ε_p, and δ_p are specified, allowing the solution of Eq. (31) to find the value of ρ_a. However, for the conditions investigated in this work, there are either one or three real solutions to Eq. (31). To compute all real solutions, the method of Topliss et al. (1988) for solving non-cubic equations of state was extended to the pure fluid adsorption equilibrium problem as formulated here.

Fig. 4 shows the two shapes (labeled as α and β) observed in this work for the plot μ_a *vs.* ρ_a of a pure fluid, depending on problem specifications. A type-α plot has only one real solution to Eq. (31), whereas a type-β curve may give one or three real solutions, due to the presence of a local maximum at point $B=(\rho_a^B,\mu_a^B)$ and a local minimum at point $C=(\rho_a^C,\mu_a^C)$. Fig. 5 shows the two observed shapes of the plot $d\mu_a/d\rho_a$ *vs.* ρ_a of a pure fluid. Both plot types show a global minimum at point $A=(\rho_a^A,\mu_a^A)$, which corresponds to the inflexion point of the curves in Fig. 4. However, a type-α curve has a positive minimum, whereas a type-β curve has a negative minimum. Therefore, it is necessary to calculate the coordinates of point A to identify the curve type. That was done using the golden section method applied to the interval $0.001\ \rho_{max}>\rho_a>0.9\ \rho_{max}$.

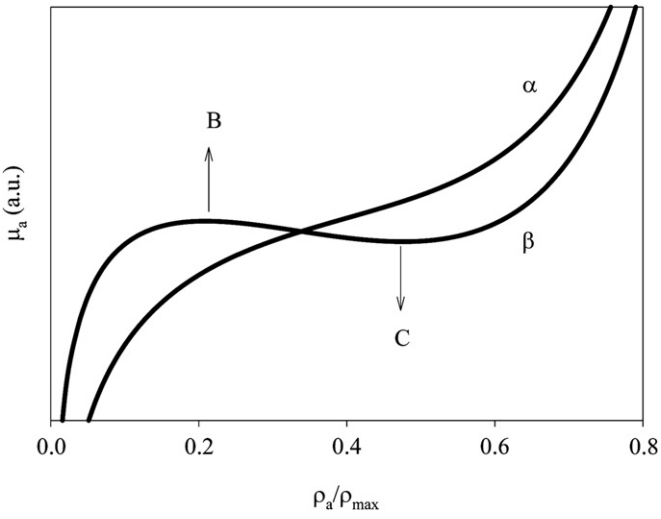

Fig. 4. Possible shapes of the curve μ_a *vs.* ρ_a for a pure fluid.

When a type-β curve is identified, one must calculate the coordinates of points B and C to know the number of real solutions of Eq. (31). Points B and C were calculated using the golden section method applied to the intervals $0.001\,\rho_{max} > \rho_a > \rho_a^A$ and $\rho_a^A > \rho_a > 0.9\,\rho_{max}$, respectively. If the chemical potential specification is higher than μ_a^B or lower than μ_a^C, there is only one real solution to Eq. (31); otherwise, there are three real solutions. In this case, only the lowest and the highest values of ρ_a are mechanically stable; the intermediate solution does not satisfy the mechanical stability criterion, since it is located in the region where $d\mu_a/d\rho_a < 0$ (see Appendix A).

After finding the number of real solutions of Eq. (31), each mechanically stable solution was calculated using the secant method with appropriate initial estimates. When there are two solutions, the lowest is calculated with initial estimates below ρ_a^B and the highest with initial estimates above ρ_a^C. If two solutions are mechanically stable, the globally stable solution is identified by the thermodynamic equilibrium condition that is consistent with the adsorbed phase specifications (temperature, total pore volume, and chemical potential). This condition is the maximum pressure of the adsorbed phase, as shown in Appendix B.

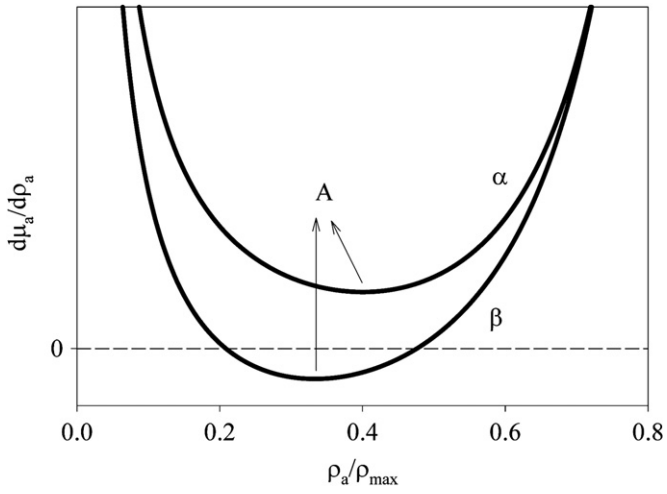

Fig. 5. Possible shapes of the curve $d\mu_a/d\rho_a$ *vs.* ρ_a for a pure fluid.

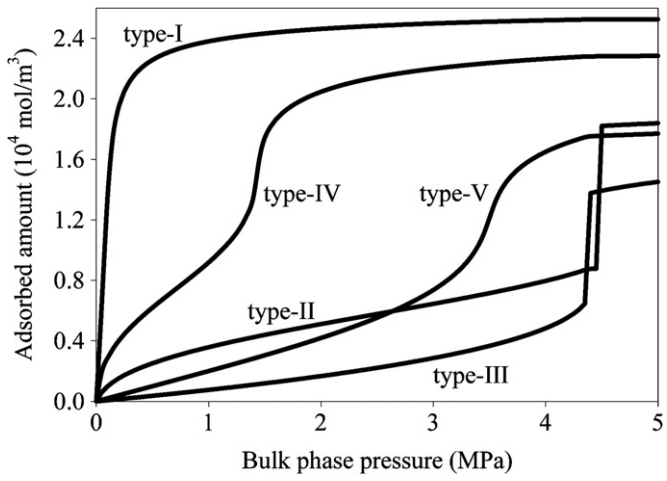

Fig. 6. CO_2 adsorption profiles computed with the parameters presented in Table 1 (T=250 K; r_p=1.5 nm).

Table 1
Parameters used to compute the isotherms in Fig. 6.

Isotherm type	ε_p/k (K)	δ_p/σ
I	1500	1.50
II	1100	0.35
III	95	3.30
IV	1500	0.65
V	500	0.65

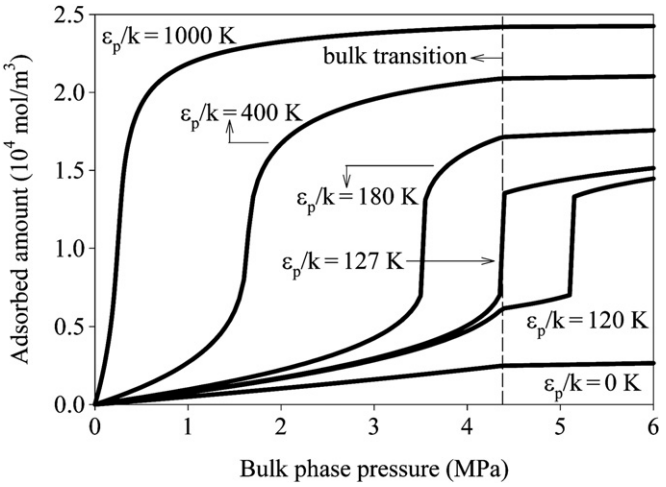

Fig. 7. CO_2 adsorption profiles for different values of parameter ε_p (T=250 K, r_p=1.5 nm, δ_p/σ=1.66).

4. Sensitivity analysis of the model for confined pure fluids

The sensitivity of the model for pure fluids to pore size and to the molecule–wall interaction parameters was analyzed. All the calculations were based on the properties of one subcritical bulk fluid: carbon dioxide at 250 K. For this compound, the parameters of the molecule–molecule interaction potential are ε/k=119 K and δ/σ=0.83 (Hirschfelder et al., 1964), given here only for comparison with the molecule–wall interaction parameters (ε_p and δ_p). Fig. 6 shows the effect of parameters ε_p and δ_p on the calculated profile of CO_2 adsorption in a nanopore with r_p=1.5 nm. The adsorbed amount is expressed per unit of pore volume. By varying the values of ε_p and δ_p, it is possible to obtain adsorption isotherms of types from I to V of the IUPAC classification (Brunauer et al., 1940). Table 1 contains the values of ε_p and δ_p used to compute each isotherm in Fig. 6.

Fig. 7 shows the effect of parameter ε_p on the calculated adsorption profile for fixed r_p=1.5 nm and δ_p/σ=1.66. The dashed line is the condition predicted by the van der Waals equation of state for the vapor–liquid transition of bulk CO_2. Depending on the value of ε_p, the model predicts either a gradual variation of the adsorbed phase density with the bulk phase pressure or the occurrence of a phase transition in the confined fluid. When the model predicts an adsorbed phase transition, it may occur at pressures below or above the bulk phase transition pressure. For low values of ε_p, the adsorbed phase transition occurs at pressures above the bulk phase transition pressure, because the repulsive effect of the molecule–wall interactions prevails. The increase of ε_p results in an increase of the adsorbed amount and a shift of the adsorbed phase transition to lower pressures, due to the increase of the attractive effect of the molecule–wall interactions. For high values of ε_p, the adsorption profile is continuous, without a phase

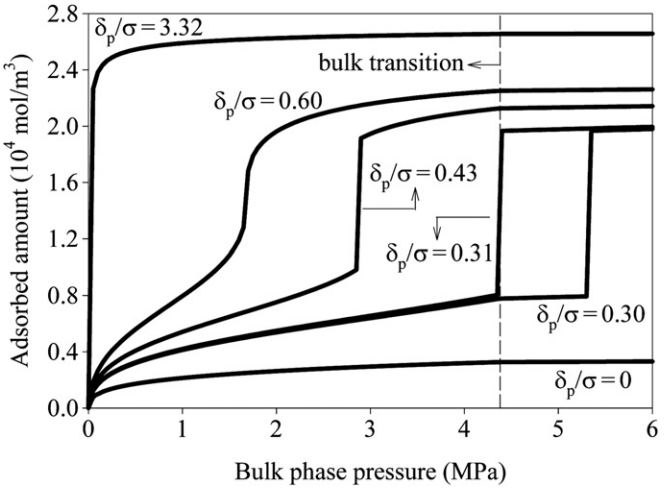

Fig. 8. CO_2 adsorption profiles for different values of parameter δ_p (T=250 K, r_p=1.5 nm, ε_p/k=1500 K).

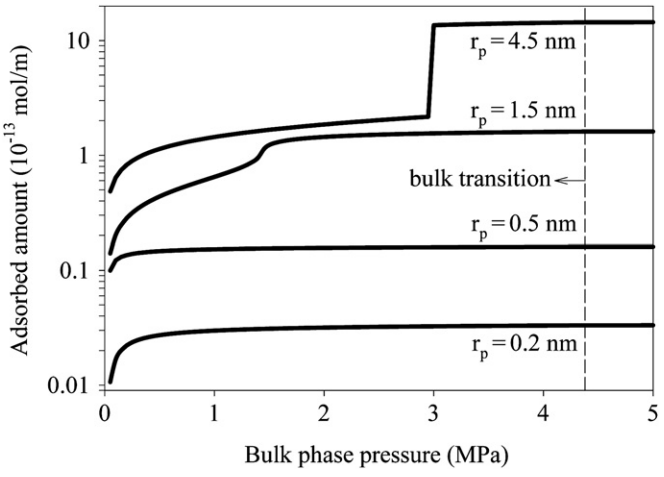

Fig. 9. CO_2 adsorption per unity of pore length for different values of r_p (T=250 K, ε_p/k=1500 K, δ_p/σ=0.65 for $r_p \geq 0.5$ nm, δ_p/σ=0.01 for r_p=0.2 nm).

transition. Regardless of the adsorption isotherm type, its slope is suddenly reduced when the bulk pressure exceeds the bulk phase transition pressure. When the bulk phase is a liquid, the effect of pressure on its properties is small. As both phases are in equilibrium, the adsorbed phase properties are also slightly influenced by the liquid bulk phase pressure, resulting in the reduction of the adsorption isotherm slope.

Fig. 8 shows the effect of parameter δ_p on the calculated adsorption profile for r_p=1.5 nm and ε_p/k=1500 K. The parameter δ_p has an effect similar to that of parameter ε_p, since both determine the intensity of the molecule–wall attraction. Therefore, the features of the adsorption isotherm (initial slope, possible occurrence of a confined fluid phase transition, and saturation pressure) depend on the values of both molecule–wall interaction parameters, which are generally strongly correlated.

Figs. 9 and 10 show the effect of pore size on the calculated adsorption profile for the case of ε_p/k=1500 K and δ_p/σ=0.65. When analyzing the effect of r_p, the parameter δ_p is specified, but its value must be in an interval with physical meaning. For a given value of r_p, δ_p may vary in the interval $0 < \delta_p < (r_p - \sigma/2)$, as can be seen in Fig. 2. When δ_p is specified, r_p must be greater than $(\delta_p + \sigma/2)$; otherwise, the entire pore interior is subjected to the wall field and the specification of δ_p must be reduced to the maximum value physically possible, $(r_p - \sigma/2)$. For example, in the case of

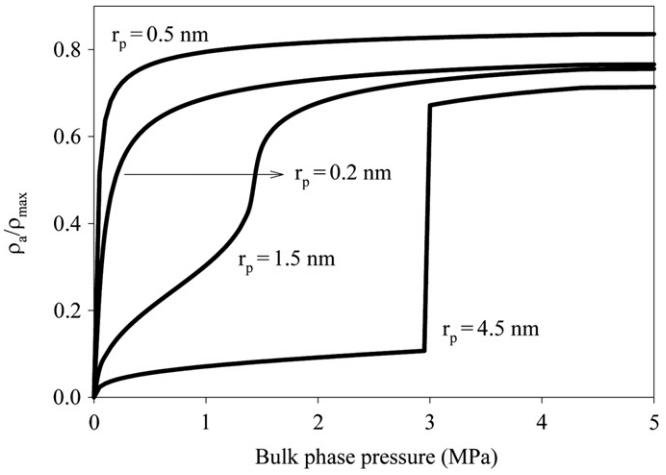

Fig. 10. Dimensionless density of confined CO_2 for different values of r_p (T=250 K, ε_p/k=1500 K, δ_p/σ=0.65 for $r_p \geq 0.5$ nm, δ_p/σ=0.01 for r_p=0.2 nm).

adsorption of CO_2 (σ=0.39 nm) in a pore with r_p=0.2 nm, δ_p/σ must be limited to 0.01.

In Fig. 9, the amount adsorbed is expressed per unit of pore length. The adsorbed amount increases with the increase of r_p, due to the increase of the available volume. For relatively large values of r_p, an adsorbed phase transition is predicted. When $r_p/\sigma \to \infty$, that transition coincides with the bulk fluid vapor–liquid transition. As r_p is reduced, the adsorbed phase transition is shifted to lower pressures due to the increase of the confined fluid fraction that is subject to the attractive field of the pore wall. For small values of r_p, an adsorbed phase transition does not occur and the adsorption profile is continuous and smooth. This is because the fluid structure becomes one-dimensional when $r_p/\sigma \to 0.5$ (extreme confinement) and a one-dimensional fluid does not undergo first-order phase transitions (Hill, 1960).

Fig. 10 shows the dimensionless density of the confined fluid, i.e. the adsorbed phase density divided by ρ_{max} (which is a function of r_p). Far from extreme confinement, the confined fluid dimensionless density increases with the reduction of r_p, due to the increase of the fluid fraction subject to the attractive field of the pore wall. When $r_p \leq (\delta_p + \sigma/2)$, all the interior of the pore is subject to the wall field, therefore the attractive effect of the molecule–wall interactions remains constant, but the repulsive effect increases with the reduction of r_p, resulting in the reduction of the confined fluid dimensionless density for high degrees of confinement.

5. Correlation of pure fluid experimental adsorption data

The model was used to correlate literature experimental data of pure fluid adsorption by fitting the molecule–wall interaction parameters (ε_p and δ_p). Parameter optimization was carried out using the Simplex method (Nelder and Mead, 1965) with the non-weighted least squares objective function. Different initial estimates of the parameters were used to increase the probability of finding the parameter set that corresponds to the global minimum of the objective function. The van der Waals parameters for pure bulk fluids (a and b) were calculated using the conventional formulas of the van der Waals equation of state model as functions of critical temperature and critical volume (Poling et al., 2000).

The model was fit to four sets of pure fluid adsorption data to evaluate its correlation performance. The first data set is the separate adsorption of methane and ethane on a MSC-5A

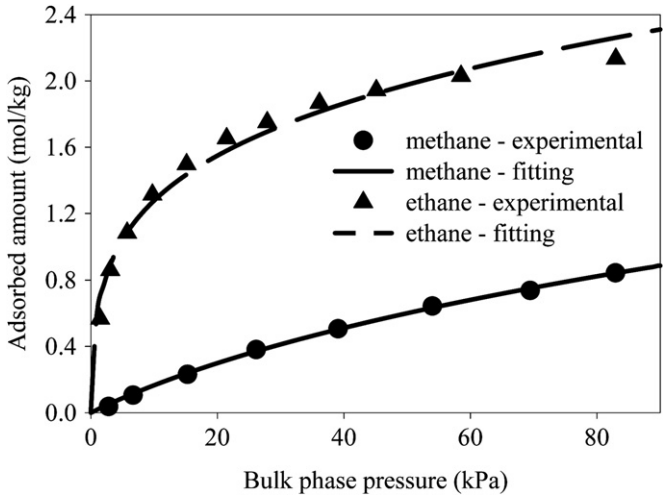

Fig. 11. Correlation of pure fluid adsorption on MSC-5A molecular sieve at 303.15 K.

Table 2
Parameters estimated from experimental data of pure fluid adsorption.

Adsorbent	Adsorbate	ε_p/k (K)	δ_p/σ
MSC-5A (r_p=1.72 nm)	methane (σ=0.398 nm)	1524.66	0.886939
	ethane (σ=0.453 nm)	3110.05	0.662325
JX-101 (r_p=0.693 nm)	methane (σ=0.398 nm)	1297.23	0.469736
	nitrogen (σ=0.386 nm)	923.261	0.402920
	hydrogen (σ=0.346 nm)	162.037	0.724385
DAY-13 (r_p=0.833 nm)	toluene (σ=0.587 nm)	4101.98	0.527783
	1-propanol (σ=0.518 nm)	4329.13	0.544490
MCM-41 (r_p=2.04 nm)	methane (σ=0.398 nm)	696.774	0.478352
	ethane (σ=0.453 nm)	997.701	1.00049

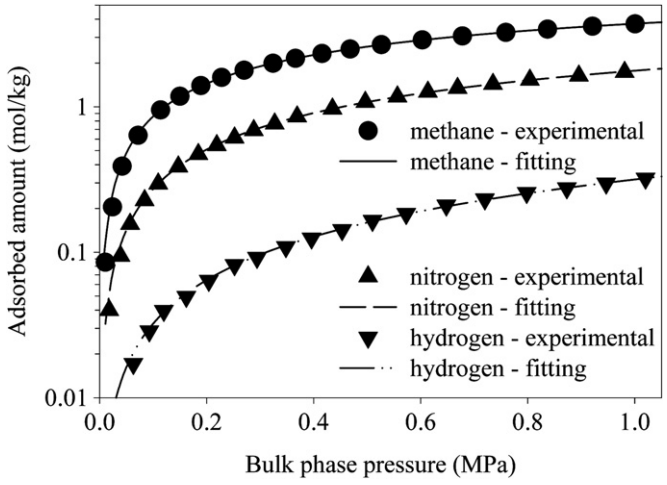

Fig. 12. Correlation of pure fluid adsorption on JX-101 activated carbon at 298 K.

molecular sieve (Konno et al., 1985; Nakahara et al., 1974). An effective pore radius of 1.72 nm was calculated from the reported values of specific area and total pore volume of the adsorbent based on the cylindrical pore assumption. Fig. 11 shows the model fit of the adsorption isotherms of the pure compounds at 303.15 K. Table 2 presents the estimated parameters for each pure component of this adsorption system, as well as of the other

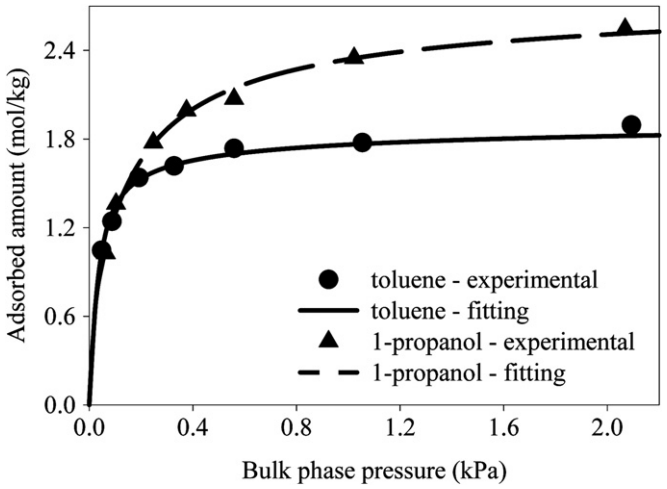

Fig. 13. Correlation of pure fluid adsorption on DAY-13 zeolite at 318.15 K.

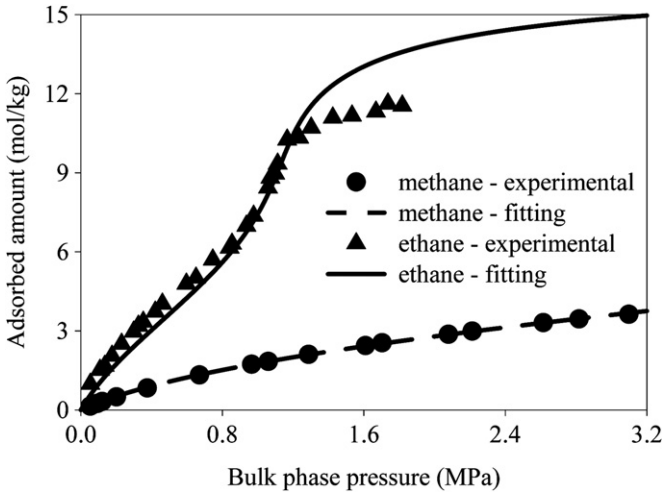

Fig. 14. Correlation of pure fluid adsorption on MCM-41 molecular sieve at 264.75 K.

adsorption systems correlated in this section. The methane isotherm was very well correlated, but slightly larger deviations were found in the correlation of the ethane isotherm, especially at the saturation region.

The second data set is the adsorption of methane, nitrogen, and hydrogen separately on a JX-101 activated carbon (Wu et al., 2005). An effective pore radius of 0.693 nm was calculated for this adsorbent, in the same way described as for the previous adsorbent. Fig. 12 shows the model fit to the adsorption isotherms of the pure gases at 298 K. Excellent correlations were obtained for all of the three isotherms.

The third data set (Sakuth et al., 1998) is the adsorption of toluene and 1-propanol separately on a dealuminated Y-zeolite (DAY-13). This adsorbent is both chemically and geometrically heterogeneous, with a net of interconnected channels of different dimensions (Giannetto, 1990). An effective pore radius of 0.833 nm was calculated for this adsorbent. Fig. 13 shows the model fit to the adsorption isotherms of the pure compounds at 318.15 K. The adsorption data of both compounds were well fit by type-I isotherms, as expected for adsorption on a microporous solid.

The last pure fluid data set is the adsorption of methane and ethane separately on a pure-silica MCM-41 molecular sieve

(Yun et al., 2002). This adsorbent is very homogeneous, both chemically and geometrically, and has a structure of long cylindrical pores with few interconnections. An average pore radius of 2.04 nm was reported for this adsorbent. Fig. 14 shows the model fitting to the adsorption isotherms of the pure compounds at 264.75 K.

The model was able to capture the IUPAC type-IV shape of the ethane isotherm (characteristic of adsorption on a mesoporous solid), but with a significant deviation in the saturation region, overestimating the maximum adsorbed amount. However, the correlation of type-IV isotherms with simple analytical models is usually unsatisfactory. Nonetheless, it is noteworthy that our model has the ability to correlate type-IV adsorption isotherms reasonably accurately.

6. Predictive calculations of mixture adsorption

Predictions of mixture adsorption were based on the correlation of pure fluid adsorption data only, with no fitting of binary interaction parameters. In each predictive calculation, the specifications are the temperature of the adsorption system, the bulk phase pressure and composition, the pore radius of the adsorbent (and its total pore volume), the van der Waals parameters and the molecule–wall interaction parameters of all fluid components. These specifications allow the solution of the system of *NC* adsorption equilibrium equations:

$$\mu_{i,b}(T, P_b, x_{1,b}, x_{2,b}, \ldots, x_{NC-1,b}) = \mu_{i,a}(T, \rho_a, x_{1,a}, x_{2,a}, \ldots, x_{NC-1,a}, r_p), \quad i = 1, 2, \ldots, NC \tag{32}$$

where $\mu_{i,b}$ and $x_{i,b}$ are the chemical potential and molar fraction of component i in the bulk phase, respectively, and $\mu_{i,a}$ and $x_{i,a}$ are the chemical potential and mole fraction of component i in the adsorbed phase, respectively. The set of Eqs. (32) was solved using the secant method to find the adsorbed phase total density and composition.

The predictive performance of the model was evaluated using the mixture adsorption data corresponding to the four pure fluid adsorption systems correlated in the previous section. The first data set is the adsorption of binary mixtures of methane and ethane on the MSC-5A molecular sieve (Konno et al., 1985). Fig. 15 shows the experimental data and the model predictions for the mixture adsorption at 303.15 K and 13.3 kPa. The model, with no additional parameters, predicted the adsorbed amount of ethane

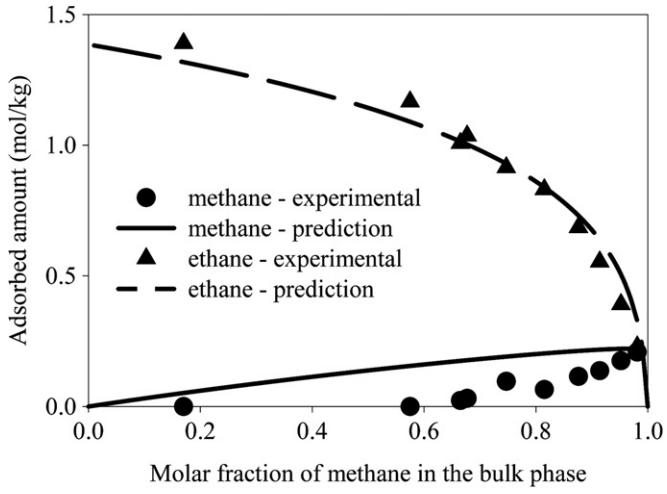

Fig. 15. Prediction of adsorption of binary mixtures on MSC-5A molecular sieve at 303.15 K and 13.3 kPa.

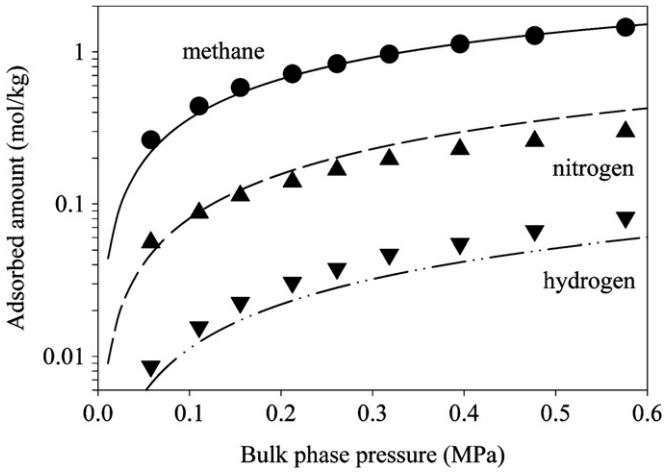

Fig. 16. Prediction of adsorption from the bulk phase ternary mixture of 36.48% methane, 27.75% nitrogen, and 35.77% hydrogen on JX-101 activated carbon at 298 K.

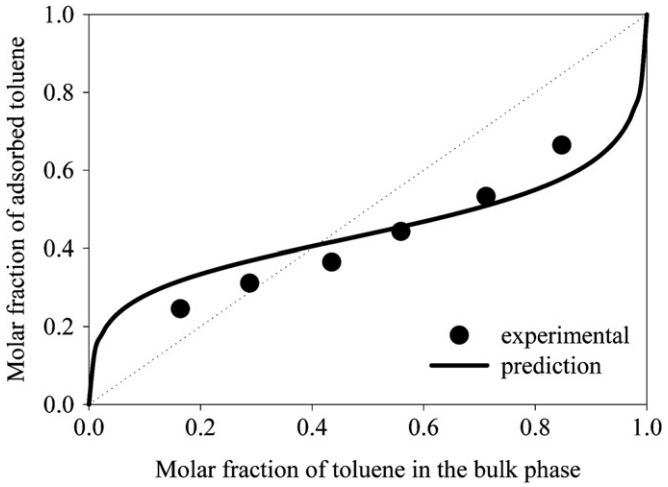

Fig. 17. Prediction of adsorption of mixtures of toluene and 1-propanol on DAY-13 zeolite at 318.15 K and 1.05 kPa.

with good accuracy, but slightly overestimated the small adsorbed amount of methane.

The second data set is the adsorption of ternary mixtures of methane, nitrogen, and hydrogen on the JX-101 activated carbon (Wu et al., 2005). Fig. 16 shows the experimental data and the model predictions for the adsorption from the bulk phase mixture of methane (36.48%), nitrogen (27.75%), and hydrogen (35.77%) at 298 K. Like the previous adsorption system, the model accurately predicted the adsorption of the component in higher concentration (methane), but resulted in somewhat larger deviations for the other components. Several predictive models evaluated by Wu et al. (2005) also resulted in lower accuracies for the calculation of the small adsorbed amount of hydrogen in this system. In this sense, our model shows a good performance in the prediction of adsorption of this ternary mixture using pure component adsorption data only.

The third data set is the adsorption of binary mixtures of toluene and 1-propanol on the DAY-13 zeolite at 318.15 K and 1.05 kPa (Sakuth et al., 1998). Fig. 17 shows the experimental data and the model predictions for this strongly non-ideal system, including a reasonably accurate prediction of the azeotropic composition. The model performance was very good, considering

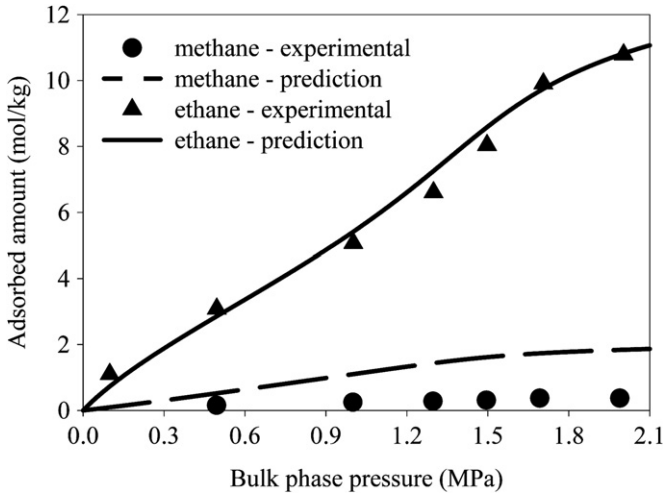

Fig. 18. Prediction of adsorption from the bulk phase binary mixture of 28.7% methane and 71.3% ethane on MCM-41 molecular sieve at 264.75 K.

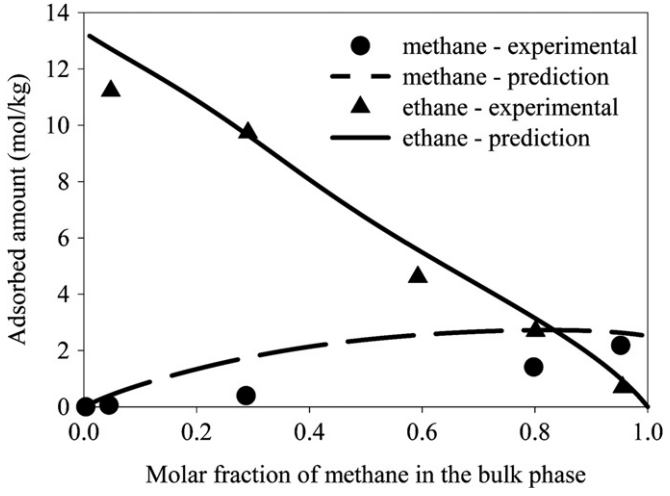

Fig. 19. Prediction of adsorption of binary mixtures on MCM-41 molecular sieve at 264.75 K and 1696.21 kPa.

that neither the chemical nor the geometrical heterogeneity of the adsorbent were taken into account in the model.

The last data set is the adsorption of binary mixtures of methane and ethane on the pure-silica MCM-41 molecular sieve (Yun et al., 2002). Figs. 18 and 19 show the experimental data and the model predictions for the mixture adsorption at 264.75 K. Fig. 18 shows the effect of pressure on the adsorption from the bulk phase mixture with 28.7% of methane and Fig. 19 shows the effect of composition on the mixture adsorption at 1696.21 kPa. In both cases, the model predicted the adsorbed amount of ethane with good accuracy, despite the deviation in the correlation of the pure ethane adsorption isotherm. Moreover, the model was able to describe the type-IV shape of the isotherms of ethane adsorption in this binary mixture. However, the adsorbed amount of methane was somewhat overestimated, similar to what was observed for the adsorption of this binary mixture on the MSC-5A molecular sieve.

7. Conclusions

The van der Waals equation of state has been extended to describe the behavior of pure fluids and mixtures confined in porous solids. The proposed model has two fitting parameters for each component of the fluid, which are related to the interaction between the fluid molecules and the pore walls. The effect of pore size on fluid properties was explicitly represented in the model, allowing its application to both confined and bulk fluids with a single set of parameters. In this way, the model provides a consistent description of adsorption systems over the whole range of pore sizes. It was found that the model can predict different adsorption isotherm shapes by varying the molecule–wall interaction parameters.

The model was found to provide good correlations of experimental data of pure fluid adsorption, including the potential to accurately describe IUPAC type-IV isotherms, despite the simplicity of the formulation. Also, the model is shown to lead to reasonable predictions of the adsorption of several binary mixtures (including one azeotropic system) and one ternary mixture, without any binary interaction parameters.

The approach presented in this work to extend the van der Waals equation of state to confined fluids can also be applied to other well known equation of state models that more accurately represent pure fluids and mixtures. For example, to extend the model to include either the Peng–Robinson or the Soave–Redlich–Kwong equation of state, it is only necessary to change the equation for the molecule–molecule coordination number. Furthermore, the effect of confinement on fluid properties related to its local structure, such as the molecule–molecule coordination number and the molecule–wall distribution function, could be investigated by molecular simulations in order to improve the formulation and performance of the model.

Notation

a	energy parameter of the van der Waals equation of state for bulk fluids
a_p	van der Waals energy parameter modified by confinement
b	volume parameter of the van der Waals equation of state for bulk fluids
b_p	van der Waals volume parameter modified by confinement
c	constant of the van der Waals expression for N_c
E_{conf}	configurational energy
F_p	fraction of the confined fluid molecules subjected to the attractive field of the pore walls
F_{pr}	value of F_p for random distribution of the fluid molecules inside the pores
G	Gibbs energy
k	Boltzmann constant
n	number of fluid moles
N	number of fluid molecules
N_{av}	Avogadro number
N_c	molecule–molecule coordination number in a pure fluid
$N_{c,ij}$	number of molecules of component i around a central molecule of component j
NC	number of components of the fluid mixture
P	pressure
q_{int}	internal partition function of one fluid molecule
Q	canonical partition function
r	distance between the mass centers of two fluid molecules
r_p	pore radius
R	ideal gas constant
s	molar entropy
S	total entropy

T	absolute temperature
u	potential of interaction between two fluid molecules
U	internal energy
v	average molar volume of the fluid
V	total volume
V_f	free volume
x	molar fraction

Greek letters

β	excluded volume per fluid molecule
δ	range parameter of the attractive interaction between two fluid molecules
δ_p	range parameter of the attractive interaction between a fluid molecule and the pore wall
ε	energy parameter of the attractive interaction between two fluid molecules
ε_p	energy parameter of the attractive interaction between a fluid molecule and the pore wall
θ	geometric term of the expression of F_p
λ	de Broglie wavelength
μ	chemical potential
μ_0	reference chemical potential
ξ	mean porosity of a packed bed of hard spheres inside a cylinder
ρ	molecular density of the fluid
ρ_{max}	molecular density of the packed fluid modified by confinement
σ	effective diameter of the fluid molecules
σ_{ij}	average molecular diameter for components i and j

Subscripts

a	adsorbed phase
b	bulk phase
i, j	components of the fluid mixture

Acknowledgments

L.T. and F.W.T. thank the financial support of CNPq and FAPERJ. M.C. thanks the support of the CAPES/Fulbright program for a Senior Visiting Professor scholarship at the University of Delaware. This research was partially supported by Grant number CTS-0083709 from the National Science Foundation.

Appendix A. Mechanical stability condition in the plane μ vs. ρ for the confined pure fluid

In a one-component system, the following relation holds:

$$d\mu = -s\,dT + v\,dP \tag{A.1}$$

where s and P are the molar entropy and the pressure, respectively. Considering the confined fluid as the system and assuming the temperature is constant, differentiation of Eq. (A.1) with respect to ρ_a gives:

$$\left(\frac{\partial \mu_a}{\partial \rho_a}\right)_T = v\left(\frac{\partial P_a}{\partial \rho_a}\right)_T \tag{A.2}$$

where the subscript a refers to the adsorbed phase. For the confined fluid to be mechanically stable, it is necessary that $\partial P_a/\partial \rho_a > 0$. According to Eq. (A.2), this mechanical stability condition can be expressed as

$$\left(\frac{\partial \mu_a}{\partial \rho_a}\right)_T > 0 \tag{A.3}$$

Relation (A.3) establishes that, when a solution of Eq. (31) results in $\partial \mu_a/\partial \rho_a < 0$, it is mechanically unstable.

Appendix B. Thermodynamic equilibrium condition for the confined fluid

In a closed homogeneous system that interacts with its surroundings only through transfers of heat or volumetric displacement work, the fluid mass is constant and the combination of the first and the second laws of Thermodynamics establishes that the system evolves to the equilibrium according to

$$dU - T\,dS + P\,dV \le 0 \tag{B.1}$$

where U and S are the internal energy and total entropy, respectively (Prausnitz et al., 1999). However, the specifications chosen in this work for the confined fluid modeling were temperature, confining volume, and chemical potential, so the fluid mass is not constant. Therefore, considering the confined fluid as the system, a term related to mass variation shall be included in Relation (B.1), which becomes:

$$dU_a - T_a\,dS_a + P_a\,dV_a - \mu_a\,dn_a \le 0 \tag{B.2}$$

where n_a is the confined fluid mole number. Considering the confined fluid specifications (T_a, V_a, μ_a), Relation (B.2) can be expressed as

$$d(U_a - T_a S_a - \mu_a n_a) \le 0 \tag{B.3}$$

From the definition of Gibbs energy:

$$G = \mu n = U + PV - TS \tag{B.4}$$

Relation (B.3) can be reduced to

$$d(-P_a V_a) \le 0 \tag{B.5}$$

As the confining volume is a specification of the adsorption equilibrium problem, Relation (B.5) reduces to

$$dP_a \ge 0 \tag{B.6}$$

Relation (B.6) establishes that the thermodynamic equilibrium condition for the confined fluid is the maximization of its pressure when the specifications are the temperature, the confining volume, and the chemical potential.

References

Brunauer, S., Deming, L.S., Deming, W.E., Teller, E., 1940. On a theory of the van der Waals adsorption of gases. Journal of the American Chemical Society 62, 1723–1732.

Coasne, B., Alba-Simionesco, C., Audonnet, F., Dosseh, G., Gubbins, K.E., 2009. Adsorption and structure of benzene on silica surfaces and in nanopores. Langmuir 25, 10648–10659.

Demontis, P., Stara, G., Suffritti, G.B., 2003. Behavior of water in the hydrophobic zeolite silicalite at different temperatures: a molecular dynamics study. Journal of Physical Chemistry B 107, 4426–4436.

Derouane, E.G., 2007. On the physical state of molecules in microporous solids. Microporous and Mesoporous Materials 104, 46–51.

Dukovski, I., Machta, J., Saravanan, C., Auerbach, S.M., 2000. Cluster Monte Carlo simulations of phase transitions and critical phenomena in zeolites. Journal of Chemical Physics 113, 3697–3703.

Giannetto, G., 1990. Zeolitas: Caracteristicas, propiedades y aplicaciones industriales. Editorial Innovación Tecnológica, Caracas.

Giaya, A., Thompson, R.W., 2002. Water confined in cylindrical micropores. Journal of Chemical Physics 117, 3464–3475.

Giovambattista, N., Rossky, P.J., Debenedetti, P.G., 2009. Effect of temperature on the structure and phase behavior of water confined by hydrophobic, hydrophilic, and heterogeneous surfaces. Journal of Physical Chemistry B 113, 13723–13734.

Hill, T.L., 1960. An Introduction to Statistical Thermodynamics. Addison-Wesley, Massachusetts.

Hirschfelder, J.O., Curtiss, C.F., Bird, R.B., 1964. Molecular Theory of Gases and Liquids. Wiley, New York.

Jiang, J., Sandler, S.I., 2006. Capillary phase transitions of linear and branched alkanes in carbon nanotubes from molecular simulation. Langmuir 22, 7391–7399.

Konno, M., Shibata, K., Saito, S., 1985. Adsorption of light hydrocarbon mixtures on molecular sieving carbon MSC-5A. Journal of Chemical Engineering of Japan 18, 394–398.

Kotdawala, R.R., Kazantzis, N., Thompson, R.W., 2005. Analysis of binary adsorption of polar and nonpolar molecules in narrow slit-pores by mean-field perturbation theory. Journal of Chemical Physics 123, 244709 (1-11).

Lee, K.-H., Lombardo, M., Sandler, S.I., 1985. The generalized van der Waals partition function–II–application to the square-well fluid. Fluid Phase Equilibria 21, 177–196.

Mueller, G.E., 2005. Numerically packing spheres in cylinders. Powder Technology 159, 105–110.

Nakahara, T., Hirata, M., Omori, T., 1974. Adsorption of hydrocarbons on carbon molecular sieve. Journal of Chemical and Engineering Data 19, 310–313.

Nelder, J.A., Mead, R., 1965. A simplex method for function minimization. Computer Journal 7, 308–313.

Nicholson, D., Parsonage, N.G., 1982. Computer Simulation and the Statistical Mechanics of Adsorption. Academic press, New York.

Poling, B.E., Prausnitz, J.M., O'Connell, J.P., 2000. The Properties of Gases and Liquids. McGraw-Hill, New York.

Prausnitz, J.M., Lichtenthaler, R.N., Azevedo, E.G., 1999. Molecular Thermodynamics of Fluid-phase Equilibria. Prentice-Hall, New Jersey.

Sakuth, M., Meyer, J., Gmehling, J., 1998. Measurement and prediction of binary adsorption equilibria of vapors on dealuminated Y-zeolites (DAY). Chemical Engineering and Processing 37, 267–277.

Sandler, S.I., 1985. The generalized van der Waals partition function–I–basic theory. Fluid Phase Equilibria 19, 233–257.

Schoen, M., Diestler, D.J., 1998. Analytical treatment of a simple fluid adsorbed in a slit-pore. Journal of Chemical Physics 109, 5596–5606.

Severson, B.L., Snurr, R.Q., 2007. Monte Carlo simulation of n-alkane adsorption isotherms in carbon slit pores. Journal of Chemical Physics 126, 134708 (1-7).

Topliss, R.J., Dimitrelis, D., Prausnitz, J.M., 1988. Computational aspects of a non-cubic equation of state for phase-equilibrium calculations: effect of density-dependent mixing rules. Computers and Chemical Engineering 12, 483–489.

Wu, J., 2006. Density functional theory for chemical engineering: from capillarity to soft materials. A.I.Ch.E. Journal 52, 1169–1193.

Wu, Q., Zhou, L., Wu, J., Zhou, Y., 2005. Adsorption equilibrium of the mixture $CH_4+N_2+H_2$ on activated carbon. Journal of Chemical and Engineering Data 50, 635–642.

Yun, J.-H., Düren, T., Keil, F.J., Seaton, N.A., 2002. Adsorption of methane, ethane, and their binary mixtures on MCM-41: experimental evaluation of methods for the prediction of adsorption equilibrium. Langmuir 18, 2693–2701.

Zarragoicoechea, G.J., Kuz, V.A., 2002. Van der Waals equation of state for a fluid in a nanopore. Physical Review E 65, 021110 (1-4).

Zarragoicoechea, G.J., Kuz, V.A., 2004. Critical shift of a confined fluid in a nanopore. Fluid Phase Equilibria 220, 7–9.

Zhu, H.Y., Ni, L.A., Lu, G.Q., 1999. A pore-size-dependent equation of state for multilayer adsorption in cylindrical mesopores. Langmuir 15, 3632–3641.